

**Rupture of molecular thin films observed in atomic force microscopy. I. Theory**Hans-Jürgen Butt<sup>1,\*</sup> and Volker Franz<sup>2</sup><sup>1</sup>*Max-Planck-Institute for Polymer Research, Ackermannweg 10, 55128 Mainz, Germany*<sup>2</sup>*Physikalische Chemie, Universität Siegen, 57068 Siegen, Germany*

(Received 19 February 2002; published 5 September 2002)

In atomic force microscope studies of molecular thin films, a defined jump of the tip through the film is often observed once a certain threshold force has been exceeded. Here, we present a theory to describe this film rupture and to relate microscopic parameters to measurable quantities. We assume that the tip has to overcome an activation energy before the film ruptures. A universal relation between the force dependence of the activation energy and the approaching velocity of the tip is derived. Two complementary models for calculating the activation energy are presented: a continuum nucleation model and a discrete molecular model. Both models predict a narrow distribution of yield forces in agreement with experimental results.

DOI: 10.1103/PhysRevE.66.031601

PACS number(s): 68.37.-d, 68.15.+e, 68.47.Pe, 64.60.Qb

**I. INTRODUCTION**

Molecular thin films on solid substrates have extensively been studied with the atomic force microscope (AFM). By imaging, for instance, lipid bilayers in aqueous medium, their molecular structure as well as their defects have been analyzed [1–7]. Besides imaging, force measurements can be done to obtain additional information. In an AFM force measurement, the tip attached to a cantilever spring is moved towards the sample. Position of the tip and deflection of the cantilever are recorded and converted to force-versus-distance curves, briefly called “force curves.” Different types of interactions, such as Derjaguin-Landau-Verwey-Overbeek (DLVO) forces, the hydration force, or steric forces have been studied with the AFM [8–10].

When measuring force curves on molecular thin films, a jump of the tip is often observed once a certain threshold force has been exceeded. Such jumps occur not only on solid supported lipid bilayers [4,11–13], but also in other systems such as surfactant layers on various substrates [14–17]. This jump is interpreted as a penetration of the AFM tip through the film. In addition, when studying confined liquids with the AFM, several jumps are often observed, which corresponds to density fluctuations. Layer after layer is squeezed out of the gap between tip and substrate. This effect was detected with fluids such as octamethyl-cyclotetrasiloxane [18], different alcohols [18–21], and liquid crystals [22].

Rupture of thin films has been analyzed extensively because of its importance for industrial and natural processes. Several mathematical models have been proposed and successfully applied to describe the destabilization of foams and emulsions [23,24], the dewetting of thin liquid films [25], the rupture of lubricant films [26], and the poration of biological membranes [27–31]. For the rupture of solid supported thin films under the influence of an AFM tip, such a model is, however, still missing. The models that are usually used to describe rupture of thin films are not directly applicable to the situation in an AFM. Reasons for this are that the mol-

ecules in the film are often insoluble and not in equilibrium with a reservoir, the position of film rupture is localized by the tip, or high pressure gradients are present.

In this paper we present a theory of film rupture induced by an AFM tip. Some ideas were presented in an earlier publication [21]. Formally, the first part is partially similar to the theory of Heymann and Grubmüller [32], Evans [49], and Tees, Waugh, and Hammer [33]. They analyze the rupture of single molecular bonds under the influence of an increasing load. The aim is to relate microscopic parameters of the film with macroscopic quantities as determined in a force measurement. In most experiments, only the threshold force for film rupture, the yield force, is reported. We show that additional information can be obtained by measuring the dependence of the yield force on the loading rate  $\nu$ . The loading rate is the approaching velocity of the base of the cantilever. From such a measurement the activation energy of the rupture process can be characterized.

The paper is divided into five sections. After the introduction, we describe the general formalism. In this part, basic equations are derived that describe the rupture kinetics in general. Besides the fact that an activation energy exists, no other assumptions are made. In the following two sections we propose two specific models for the activation process. One is a continuum nucleation theory and the other is a model that explicitly takes the molecular nature of the film into account. Both are based on the elastic foundation model (p. 104 of Ref. [34]) to calculate the pressure distribution underneath the tip. The full molecular model leads to awkward mathematical expressions in which dependencies are not obvious. Therefore, in the last section we derive a simplified molecular model, which still contains the main features but leads to much simpler expressions. We show that it is a good approximation of the full molecular model.

Throughout the paper we use the term “film,” though for some applications “layer” might have been more appropriate. The films considered are one or few molecules thick and are supposed to show a distinct structure in normal direction. Laterally, the film can be fluid with a high mobility of the molecules. Two-dimensional fluid films are characterized by an attractive interaction between the molecules. This is, for instance, the case for lipid bilayers in aqueous electrolyte.

\*Author to whom correspondence should be addressed. FAX: +49-271-740 3198; email address: butt@chemie.uni-siegen.de

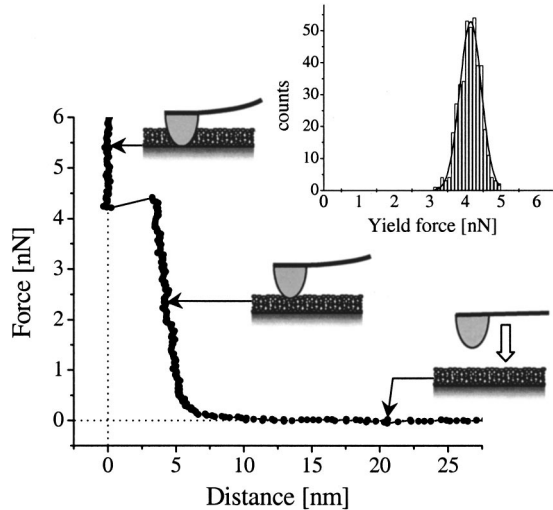


FIG. 1. A typical approach part of a force curve measured on a lipid bilayer of dioleoyloxypropyl-trimethylammonium chloride (DOTAP) on mica with a standard silicon nitride tip in aqueous buffer (150 mM NaCl, 5 mM  $\text{KH}_2\text{PO}_4$ , pH 7.4) taken at  $2 \mu\text{m/s}$  loading rate. The lipid bilayer was formed by spontaneous vesicle fusion. For details see Ref. [21]. The inserted histogram shows the number of yield forces observed in a series of experiments.

There, the film even heals out after being penetrated by an AFM tip. For the nucleation model the fluidity of the film is a prerequisite. The molecular model is more general: Neither the two-dimensional fluidity nor the lateral interaction between molecules is assumed. Only an attractive force between the solid substrate and the film molecules is required (otherwise the film would not remain on the substrate). Therefore, even layers of adsorbed immobile molecules can be treated with the molecular approach.

Before starting, it is instructive to consider a typical force curve measured on a thin film to justify certain assumptions (Fig. 1). The force curve was recorded on a lipid bilayer of  $\approx 4 \text{ nm}$  thickness. No interaction is observed at distances much larger than the film thickness. At closer distances the tip experiences a short-range repulsive force and the film is elastically compressed. Here, “elastic” refers to the fact that when retracting the tip before the film ruptures, the retracting part of the force curve is identical to the approaching part. Finally the film ruptures, and the tip jumps onto the solid support.

## II. GENERAL FORMALISM

### A. Assumptions

First, one important general observation is that the jump of the tip through the film is fast. The time required for the jump is only limited by the resonance frequency of the cantilever (typically 5–50 kHz). The hydrodynamic flow of the film material or surrounding liquid out of the closing gap between the tip and solid support is not limiting the breakthrough. Thus, we assume that the rupture process itself is infinitely fast.

Second, we assume that the rupture is a statistical process and we have to describe the process in terms of probability.

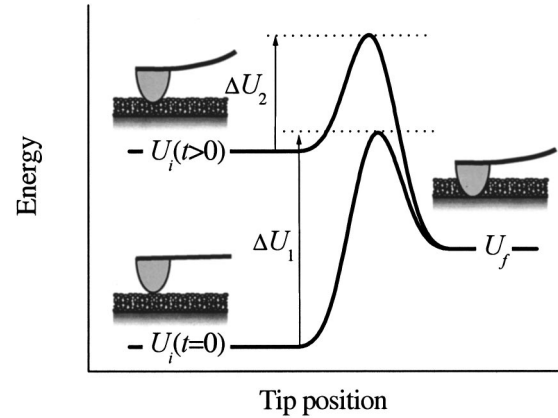


FIG. 2. Schematic representation of the energy of the molecular film (drawn as a lipid bilayer) underneath an AFM tip vs the distance of the tip. In general, this profile changes with the applied force. With increasing force the pressure applied to the film increases. During this pressure increase, the activation energy is reduced from  $\Delta U_1$  to  $\Delta U_2$  although the tip is still positioned on top of the film.

The tip on top of the thin film has a certain probability to break through the film. This probability per unit time increases with increasing force and applied pressure. Thus, there is a distribution of yield forces and not one definite value.

Third, we describe the rupture of the film and the yield as an activated process. An energy barrier has to be overcome in the process (Fig. 2). This is the activation energy for the formation of a hole in the film, which is large enough to initiate tip penetration. In detail, this process can be divided into several steps. Before the tip approaches the film both are well separated and no force is acting on the tip. The energy of this initial state of the lipid film underneath the tip is  $U_i$ . We neglect short- and long-range forces and assume that the tip at a distance  $z=h$  gets into contact with the surface of the film. Here,  $z$  is the distance between tip and sample, and  $h$  is the film thickness. At this point, the energy of the film is still  $U_i$ . When the base of the cantilever moves further down, the cantilever is deflected and the tip exerts a force on the film. At this point, we do not need to specify the nature, height, and shape of the energy barrier. It is only important to note that the applied force reduces the energy barrier. The film becomes unstable under the pressure and a rupture becomes more likely. After the tip has penetrated the film, it gets into direct contact with the solid support. At this position,  $z=0$ , the energy of the lipid film is  $U_f$ .

In our model we do not specify the distance dependency  $U(z)$  except that  $U(z=h)=U_i$  and  $U(z=0)=U_f$ . Once the tip got into contact with the film at  $t=0$ , the pressure on the film increases and thus  $U_i$  increases. An increase in  $U_i$  reduces the activation energy, which increases the probability of a film rupture. If the activation barrier is of the order of  $k_B T$ , the reaction quickly occurs once it has become thermodynamically favorable ( $U_f < U_i$ ). Here,  $k_B$  and  $T$  are Boltzmann’s constant and temperature.

### B. Kinetics of rupture

In order to describe the rupture mathematically we consider an ensemble of  $N_0$  identical AFM force experiments. Every AFM tip exerts a growing force on a film. After a time  $t$  has elapsed,  $N$  films remain intact (no rupture). For  $U_f > U_i$ , the tip cannot jump through the film. We have to wait until the pressure has increased so that the final energy becomes lower than the initial energy ( $U_f \leq U_i$ ). The “starting” time, that is, the time when the force applied by the tip has increased  $U_i$  so that the condition  $U_f \leq U_i$  is fulfilled, is denoted by  $t_S$ . If at the first contact the condition  $U_f \leq U_i$  is already fulfilled, we have  $t_S = 0$ .

Within the time interval  $dt$  the number of tips on top of the film is reduced by  $dN$  since  $|dN|$  tips penetrate through the film.  $|dN|$  is proportional to the number of intact layers  $N$ , a rate constant  $k$ , and the time interval  $dt$ :  $dN = -kNdt$ . In general,  $k$  is time dependent. Dividing by  $N_0$ , we change to probabilities

$$dP = -k(t)P dt, \quad (1)$$

where  $P = N/N_0$  is the probability of finding a tip on top of the intact film. For  $t \leq t_S$ , we have  $P = 1$ . Differential Eq. (1) can be integrated,

$$\ln P(t) = - \int_{t_S}^t k(t') dt' \quad \text{for } t > t_S. \quad (2)$$

Now we assume that the rate constant  $k$  is associated with an activated process and follows an Arrhenius law. The probability for film rupture by thermal fluctuations is proportional to the Boltzmann factor

$$k(t) = A e^{-\Delta U(t)/k_B T}. \quad (3)$$

Here,  $\Delta U$  is the activation energy necessary for the formation of a hole in the film that is large enough to initiate rupture and let the tip break through.  $A$  is the frequency at which the tip “attempts” to penetrate the film.

Film rupture and breakthrough of the tip are usually represented in terms of force rather than in terms of time. Neglecting long- and short-range interactions, the force is zero until the tip comes into contact with the film. Then, since the base of the cantilever is moved at a constant velocity  $\nu$  towards the sample, the load increases according to  $F = K\nu t$ . Here,  $K$  is the spring constant of the cantilever and  $F$  is the force applied at a time  $t$ . Substitution leads to

$$\ln P(F) = - \frac{A}{K\nu} \int_{F_S}^F e^{-\Delta U(F')/k_B T} dF' \quad \text{for } F > F_S. \quad (4)$$

$F_S = K\nu t_S$  is the “starting” force applied by the tip at  $t = t_S$ .

### C. Mean yield force and approaching velocity

In this subsection we discuss the question: Is it possible to measure how the activation energy  $\Delta U$  depends on the applied load  $F$ ? To address this question we first introduce the mean yield force  $F_0$ . All experiments showed that the rela-

tive width of the distribution of yield forces (see insert Fig. 1) is small:  $\Delta F/F_0 \ll 1$  ( $\Delta F$  is the half width of the yield force distribution). In this case, the mean yield force is similar to the force at which the probability is one half:  $P(F_0) = 0.5$ . With  $\ln 0.5 = -0.693$ , we can write

$$\nu = \frac{A}{0.693K} \int_{F_S}^{F_0} e^{-\Delta U(F)/k_B T} dF. \quad (5)$$

Since the integral increases monotonically with  $F_0$ , Eq. (5) directly shows that  $\nu$  is a monotonically increasing function of  $F_0$  and vice versa: the mean yield force increases with the loading rate. The reason is intuitively understandable: The loading rate determines how fast the force on the film increases. If the force increases slowly, then in any interval  $F \dots F + \Delta F$  there are many chances for the film to rupture. At a high loading rate, there is only a little time for film rupture in a given force interval  $F \dots F + \Delta F$ , and the film has a higher chance to remain intact.

Differentiation and rearranging Eq. (5) leads to

$$\Delta U(F_0) = -k_B T \ln \left( \frac{0.693K}{A} \frac{d\nu}{dF_0} \right). \quad (6)$$

Equation (6) shows that from a measurement of the velocity dependence of the mean yield force  $\nu(F_0)$ , one can obtain  $d\nu/dF_0$  and calculate how the activation energy depends on the force. Since  $\nu$  and  $F_0$  are easy to measure, this is an important equation. We would like to point out that Eq. (6) does not refer to a specific model. In particular, we did not assume anything about the nature of the activated process.

## III. CONTINUUM NUCLEATION THEORY

In the following sections we present two specific models to describe the activation process. The first one is a continuum nucleation model.

### A. Description of the model

We consider a molecular thin, homogeneous film confined between the solid substrate and the solid surface of the tip. The tip shape is taken to be parabolic at its end with a radius of curvature  $R$ . The film is supposed to be, laterally, in a liquid state, but vertically its structure is well defined. Assume that due to thermal fluctuations a small circular hole of radius  $r_h$  is formed in the two-dimensional fluid layer under the tip. The energy of such a hole is

$$U = 2\pi r_h \Gamma + \pi r_h^2 \left( S - \frac{F}{2\pi R} \right). \quad (7)$$

The first term,  $2\pi r_h \Gamma$ , represents the free energy associated with the unsaturated bonds of the molecules at the periphery of the hole.  $\Gamma$  is the line tension. The second term,  $\pi r_h^2 S$ , is the change in interfacial free energy. It is proportional to the area of the hole. We call the parameter  $S$  “spreading pressure” because it can be used to quantify the tendency of the film to spread into the gap between the tip and substrate.  $S$  is

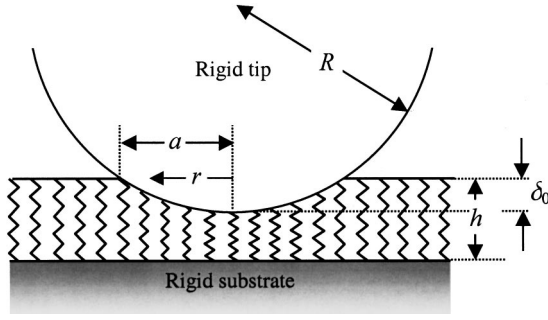


FIG. 3. Schematic drawing of a film resting on a rigid solid support which is compressed by a rigid tip.

determined by several interfaces. Assuming that the experiment is done in liquid, we denote by  $\gamma_{TF}$  the energy of the tip-film interface, by  $\gamma_{TL}$  the energy of the tip-liquid interface, by  $\gamma_{SF}$  the energy of the substrate-film interface, and by  $\gamma_{SL}$ , the energy of the substrate-liquid interface. Upon hole formation, tip-film and substrate-film interfaces are replaced by the corresponding interfaces with the liquid and we have  $S = \gamma_{TL} + \gamma_{SL} - \gamma_{TF} - \gamma_{SF}$ . For an experiment in gaseous environment, the index “L” has to be replaced by “G.” The first two terms are often used to describe hole formation in lipid bilayer membranes in electroporation [30,31] in the osmotically induced permeation of vesicles or cells [27,29,35,36], or, in general, in black films [37].

Until now, our treatment is almost similar to the theory of Persson and Tosatti [38]. As a third term, Persson and Tosatti inserted the elastic relaxation energy of the two solid surfaces upon hole formation. Instead, we consider the elastic energy of the confined film. The reason for this is that for a typical AFM experiment the elastic constants of tip and substrate are much higher than the elasticity of the film. Therefore, upon compression more elastic energy is stored in the film than in the confining solids.

To calculate the elastic energy of the film we use the elastic foundation model. In the elastic foundation or “mattress” theory, the film is modeled by many springs that do not interact, i.e., shear between adjacent springs is ignored (Fig. 3) [34]. The effective spring constant per unit area is  $E/h$ , with Youngs modulus  $E$ . One may argue that a mattress model is not adequate to describe a fluid film because in the film the molecules might tilt or can move laterally. Experiments, however, clearly indicate that before rupture occurs the response of the film is elastic. We cannot discriminate if the molecules tilt or are really compressed. This, however, is not relevant as long as the process is elastic. Also, a slight thinning of the film cannot be excluded (which in the model corresponds to a reduction of springs per unit area). Again, this would only lead to a small correction, which we ignore in this study. For these reasons, Youngs modulus should be interpreted as an effective value.

In the elastic foundation model the indentation  $\delta$  at a given radial position  $r$  is given by

$$\delta = \delta_0 - \frac{r^2}{2R} \quad (8)$$

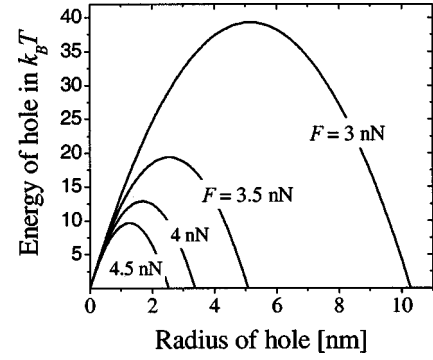


FIG. 4. Energy of a hole  $\Delta U$  of radius  $r_h$  calculated with Eq. (7) with  $\Gamma = 10^{-11}$  N,  $S = 0.01$  N/m, and  $R = 40$  nm.

for  $r \leq a = \sqrt{2\delta_0 R}$ . Here,  $a$  is the peripheral radius of the contact area. The maximal indentation in the center  $\delta_0$  and the applied force  $F$  are related by

$$\delta_0 = \sqrt{\frac{hF}{\pi ER}}. \quad (9)$$

We can calculate the elastic energy stored in a small section of the film of radius  $r_h$ . If the considered area is much smaller than the contact area ( $r_h \ll a$ ), this elastic energy is

$$\pi r_h^2 \frac{E}{h} \frac{\delta_0^2}{2} = \pi r_h^2 \frac{F}{2\pi R}. \quad (10)$$

Upon formation of a hole of radius  $r_h$ , this energy is released, hence the minus sign in Eq. (7).

It is reasonable to assume that the line tension  $\Gamma$  and the spreading pressure  $S$  are positive. If  $\Gamma$  was negative, large holes should form spontaneously. For negative  $S$ , the film would probably not adsorb to the substrate. Applying a force reduces the energy  $U$ . Once the force exceeds  $2\pi RS$ , the energy  $U(r_h)$  shows a maximum at a certain critical radius  $r_c$  (Fig. 4),

$$r_c = \frac{2\pi R\Gamma}{F - 2\pi RS}. \quad (11)$$

The maximal energy, which is the activation energy, is given by

$$\Delta U = U(r_c) = \frac{2\pi^2\Gamma^2 R}{F - 2\pi RS}. \quad (12)$$

This maximal energy decreases with increasing force. Holes with larger radius than  $r_c$  are likely to have an increase in size, a film rupture, and a tip breakthrough.

## B. Results and discussion

With respect to a comparison with experimental results, the distribution of yield forces is determined. Therefore, we start by calculating  $P(F)$  with Eq. (4),  $F_S = 2\pi RS$ , and by inserting expression (12) for  $\Delta U$ ,



$$\ln P(F) = -\frac{A}{K\nu} \int_{F_S}^F \exp\left(-\frac{2\pi^2\Gamma^2 R}{F' - F_S}\right) dF'. \quad (13)$$

The distribution of yield forces is given by  $|dP/dF|$ . The integral does not lead to a simple analytical expression and we solved it numerically.

What are reasonable values for the parameters to be inserted? The “macroscopic” parameters determined by the experimental setup are  $K$ ,  $\nu$ , and  $R$ . Spring constants are typically in the range of 0.5–0.05 N/m; we use an average value of  $K=0.1$  N/m. Loading rates are limited by a possible drift [39] (lower limit) and by hydrodynamic effects of the cantilever [40] (upper limit). Practically, a range between  $\nu = 10$  nm/s and  $100 \mu\text{m/s}$  is accessible. The radius of curvature of the tip is typically 10–80 nm depending on the fabrication process. We use a value of  $R=40$  nm. Reasonable microscopic parameters ( $\Gamma$ ,  $S$ , and  $A$ ) are more difficult to estimate. Line tensions for solid-liquid-vapor systems were calculated and experimentally verified to be in the range of  $10^{-12}$  and  $10^{-10}$  N [41,42]. Values between  $10^{-11}$  and  $10^{-10}$  N are obtained when estimating  $\Gamma$  from the product of the film-liquid (or film-gas) interfacial energy and the thickness of the film. Here, we use a value of  $\Gamma=10^{-11}$  N. Interfacial energies ( $\gamma_{TL}$ ,  $\gamma_{TF}$ ,  $\gamma_{SL}$ ,  $\gamma_{SF}$ ) are typically in the range of 0.01 to 0.1 N/m. Since  $S$  is the difference between two pairs we estimate it to be of the order of 0.01 N/m. The frequency factor  $A$  is a free parameter. An upper limit is probably given by the resonance frequency of the cantilever of typically  $10^4$  Hz. The frequency factor  $A$  cannot be significantly higher than the resonance frequency because even if holes form with a higher frequency, the tip would not be able to use them for a breakthrough.

For an easier comparison with experimental results, Fig. 5(a) shows the yield probability  $|dP/dF|$  instead of  $P(F)$ . As parameters we chose  $A=10$  kHz and  $\nu=1 \mu\text{m/s}$ . The rupture probabilities are of the same order as those observed experimentally and the same typical narrow peak is obtained. With increasing spreading pressure  $S$ , the yield force increases linearly while the shape of the probability distribution remains the same. When varying the frequency factor  $A$  and keeping  $S=0.01$  N/m fixed [Fig. 5(b)], the shape of the probability distribution changes: With decreasing  $A$  the width of the peak increases. In addition, the mean yield force is reduced with increasing  $A$  [inset of Fig. 5(b)].

One could use the width of the peak in  $|dP/dF|$  as a quantity to test the theory. Experimentally this is, however, not so simple because different sources of error in the experiment might lead to an increase of the width. Unless noise is negligible in the experiment the only condition is that the width of the theoretical peak should be smaller than or equal to the experimental peak. Thus, the width of the peak is practically often not a useful criterion to verify a theory. A more useful test is a comparison of the graph  $F_0$  vs  $\nu$ . Using Eq. (5) we can calculate how the mean yield force  $F_0$  depends on the loading rate  $\nu$  [Fig. 5(c)]. The results show a monotonic increase. For low loading rates,  $F_0$  is almost con-

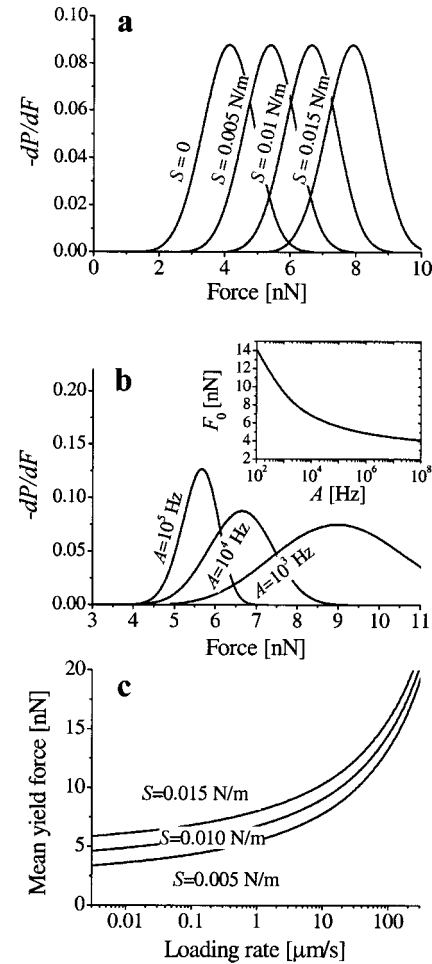


FIG. 5. (a) Probability of a rupture  $|dP/dF|$  as derived with the nucleation model Eq. (13) using  $A=10^4$  Hz,  $K=0.1$  N/m,  $\nu=1 \mu\text{m/s}$ ,  $\Gamma=10^{-11}$  N, and  $R=40$  nm for different values of the spreading pressure  $S$ . (b) Probability of rupture for different values of the frequency factor  $A$  with  $S=0.01$  N/m. The inset shows how the mean yield force  $F_0$  decreases with increasing frequency factor  $A$ . (c) Dependence of the mean yield force  $F_0$  on the loading rate  $\nu$  for  $A=10^4$  Hz and different values for  $S$ .

stant, for high loading rate  $F_0$  increases. With increasing spreading pressure the curves are shifted to higher mean yield forces.

## IV. MOLECULAR MODEL

### A. Description of the model

The approach is related to the model developed by Galla *et al.* [43], which refers to an earlier idea of Cohen and Turnbull [44]. In the molecular model each molecule in the film has certain binding sites that are energetically favorable positions. These binding sites might be formed by the substrate or by the surrounding molecules. To jump from the initial position into an adjacent free position a potential energy barrier has to be overcome (Fig. 6). In the absence of the tip, adjacent binding sites are energetically equivalent. When the tip is pressed onto the film a pressure gradient is applied, which increases the energy of the molecules. The pressure is

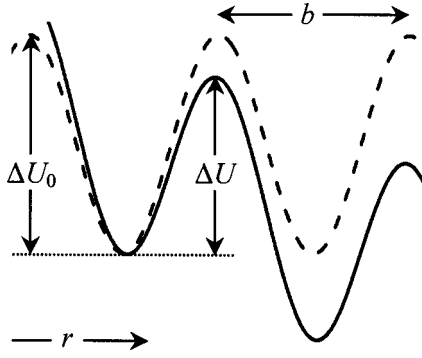


FIG. 6. Schematic representation of the energy vs radial distance of a molecule in the film with (continuous line) and without (dashed line) a pressure gradient due to the tip pressure. Such an energy profile was used for the molecular model.

maximal in the center of the tip and it decreases with increasing radial distance  $r$  until it becomes zero at the contact periphery at  $r=a$ . At the same time, this pressure gradient lowers the activation barrier. This idea—a lowering of the activation energy by changing the energy level of the initial or final state—is already applied to analyze such diverse phenomena like an electric current in a Josephson tunnel junction [45] or ion currents through biological membranes [46].

What is the “compression” energy of a molecule? The surface area occupied by one molecule in the film is  $\approx \lambda^2$  with  $\lambda$  as the lateral distance between adjacent molecules. In the elastic foundation model each segment of the film of area  $\lambda^2$  acts like a spring with a spring constant  $\lambda^2 E/h$ . If this segment is compressed by an indentation  $\delta$  the elastic energy increases to  $\lambda^2 E \delta^2/2h$ . Thus, the additional energy of a molecule due to the pressure of the tip is

$$u = \frac{E\lambda^2}{2h} \left( \delta_0 - \frac{r^2}{2R} \right)^2. \quad (14)$$

Molecules are most likely to jump (and form a hole) where the difference in energy between adjacent binding sites is maximal. In that case the energy release is the highest. This is at the maximum of the energy gradient  $du/dr$  at  $r = \sqrt{2} \delta_0 R/3$ . Differentiating Eq. (14) and inserting Eq. (9) we get a maximal energy gradient for a molecule to be

$$\left. \frac{du}{dr} \right|_{\max} = \frac{\lambda^2}{R} \left( \frac{2}{3} \right)^{3/2} \left( \frac{EF^3}{\pi^3 hR} \right)^{1/4}. \quad (15)$$

To obtain the effective activation energy we take the energy gain of a molecule jumping from  $r = \sqrt{2} \delta_0 R/3$  to an adjacent site at  $r = \sqrt{2} \delta_0 R/3 + \lambda$  as  $\Delta u = \lambda du/dr|_{\max}$ .

In general, for the formation of a hole large enough to initiate tip breakthrough, a certain critical number of molecules  $n$  is required. Once these molecules have left the contact area the force applied by the tip is distributed among fewer molecules. This increases the pressure gradient and thus the chance of the remaining molecules to jump to larger  $r$  and also escape from under the tip. The “activation volume” of these  $n$  molecules is  $V = n\lambda^2 h$ , assuming the film is a monolayer (for a double layer it is  $V = 2n\lambda^2 h$ , for three

layers it is  $V = 3n\lambda^2 h$ , etc.). Taking this into account, the initial activation energy (without an applied force)  $\Delta U_0$  is reduced by the force according to

$$\Delta U = \Delta U_0 - \alpha \frac{V\lambda}{hR} \left( \frac{2}{3} \right)^{3/2} \left( \frac{EF^3}{\pi^3 hR} \right)^{1/4}. \quad (16)$$

The factor  $\alpha$  is a geometrical factor. It takes into account that the reduction of the activation energy might be lower than the change in energy between adjacent sites. For a symmetrical barrier it should be  $\alpha = 0.5$ , provided that the contact radius is much larger than the distance between adjacent binding sites (practically for  $R \gg \lambda$ ). Inserting expression (16) into Eq. (4) leads to

$$\ln P(F) = - \frac{k_0}{K\nu} \int_0^F \exp \left[ \left( \frac{F'}{F_M} \right)^{3/4} \right] dF', \quad (17)$$

with a rate  $k_0 \equiv A \exp(-\Delta U_0/k_B T)$  and

$$F_M \equiv \frac{9\pi}{4} \left( \frac{k_B T h R}{\alpha V \lambda} \right)^{4/3} \left( \frac{hR}{E} \right)^{1/3}. \quad (18)$$

The lower integration limit was set to zero ( $F_5 = 0$ ) because the energies of adjacent binding sites are equivalent before the tip exerts a force. Integration of Eq. (17) does not lead to a simple algebraic expression and was done numerically.

## B. Results and discussion

What is a reasonable range for the parameter  $F_M$ ? Effective Youngs moduli for lipid layers range from 2 MPa–10 GPa as determined from electroporation experiments [31] and by acoustic Brillouin scattering of Langmuir-Blodgett multilayers [47], respectively. For individual layers of alcohols, effective Youngs moduli are between  $10^7$ – $10^8$  Pa [48]. An upper limit of  $F_M$  can be estimated by assuming that the activation volume is only a single molecule of volume  $V = h\lambda^2$ . Then, with  $h = 4$  nm,  $\lambda = 0.5$  nm (resulting in  $V = 1$  nm<sup>3</sup>),  $\alpha = 0.5$ , and  $E = 2$  MPa, the upper limit is  $F_M \approx 1.1$   $\mu$ N. For the lower limit we insert a hundred times larger volume,  $h = 1$  nm, and  $E = 10$  GPa and obtain  $F_M \approx 50$  pN.

A series of results for the yield probability  $|dP/dF|$  is shown in Fig. 7(a). The parameters were  $k_0 = 0.1$  Hz and  $\nu = 1$   $\mu$ m/s. In agreement with typical experimental results (see Fig. 1), the model predicts a distribution of yield forces centered in a peak. Increasing  $F_M$  leads to an increase in the yield force. Changing the rate  $k_0$  also changes the probability of a yield: An increase in  $k_0$  decreases the mean yield force, a decrease leads to a higher yield force [Fig. 7(b)].

The second criterion to verify a model is the dependence of the yield force on the loading rate. Inserting Eq. (16) into Eq. (5), we get

$$\nu = \frac{k_0}{0.693K} \int_0^{F_0} \exp \left[ \left( \frac{F}{F_T} \right)^{3/4} \right] dF. \quad (19)$$

The result is plotted as a graph of  $F_0$  vs  $\nu$  in Fig. 7(c).  $F_0$  is roughly proportional to  $\ln \nu$ , which agrees with experimental

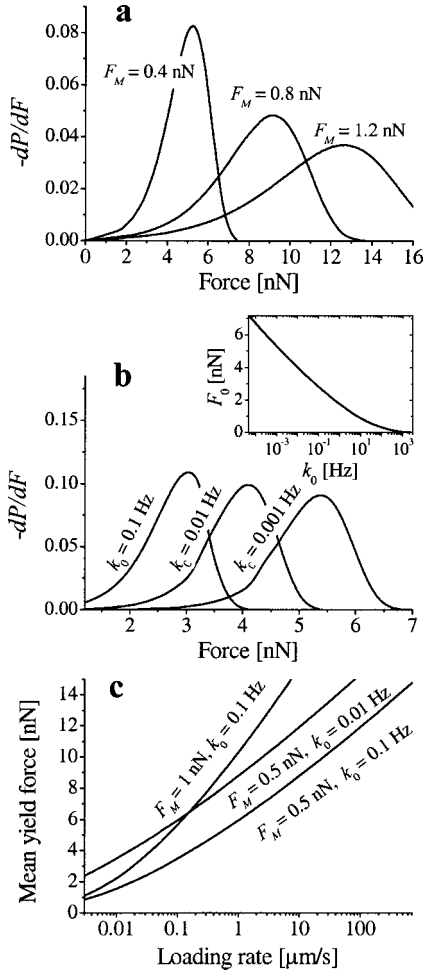


FIG. 7. (a) Probability of a rupture  $|dP/dF|$  as derived with the molecular model Eq. (17) using  $k_0=0.1$  Hz,  $\nu=1$   $\mu\text{m/s}$ ,  $K=0.1$  N/m,  $R=40$  nm for different values of  $F_M$ . (b) Probability of rupture for different values of the rate  $k_0$  keeping  $F_M=0.2$  nN fixed. The inset shows how the mean yield force  $F_0$  depends on the rate  $k_0$  for  $\nu=1$   $\mu\text{m/s}$ . (c) Dependence of the mean yield force on the loading rate calculated with Eq. (19) for different combinations of  $k_0$  and  $F_M$ .

results on lipid bilayers [21]. Increasing  $F_M$  leads to a steeper increase of the  $F_0$  vs  $\nu$  curve. Decreasing  $k_0$  shifts the curve to higher forces almost parallel to the original curve.

## V. SIMPLIFIED MOLECULAR MODEL

### A. Description of the model

The advantage of the molecular model is that it seems to describe the experimental results obtained on films adequately and that it relates microscopic parameters to measurable quantities. The disadvantage is that the results are mathematically awkward because of the integral  $\int \exp(x^{3/4}) dx$ . It would help to have a simple approximation that still contains the main features and dependencies but leads to analytical solutions. Therefore, we consider the elastic energy of a molecule in the center of the contact area, which is compressed by  $\delta_0$ . This energy is  $u_0 = E\lambda^2 \delta_0^2 / 2h$ . It

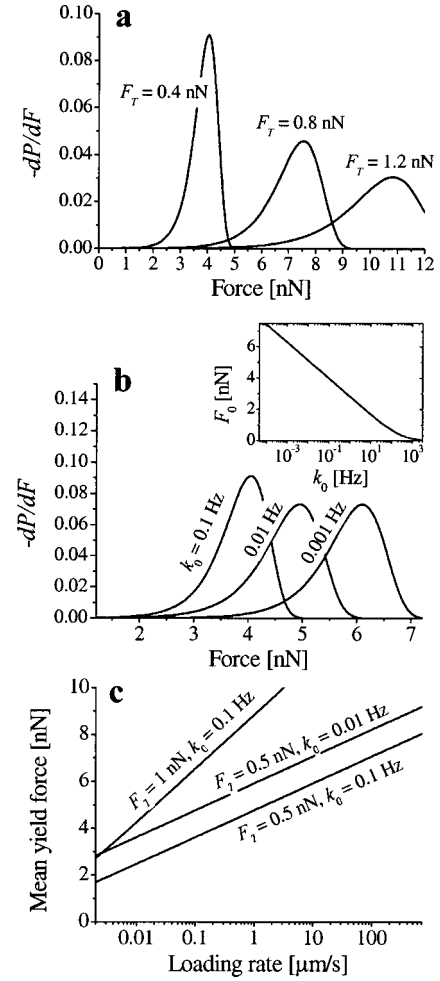


FIG. 8. (a) Probability of a rupture  $|dP/dF|$  as derived with the simple molecular model Eq. (21) using  $k_0=0.1$  Hz,  $K=0.1$  N/m,  $\nu=1$   $\mu\text{m/s}$ , and  $R=40$  nm for different values of the thermal force  $F_T$ . (b) Probability of a rupture for different values of the rate  $k_0$  at fixed  $F_T=0.5$  nN. All other parameters were as before. The inset shows how the mean yield force  $F_0$  depends on the rate  $k_0$  for  $\nu=1$   $\mu\text{m/s}$ . (c) Dependence of the mean yield force of the loading rate calculated with Eq. (23) for three different combinations of  $k_0$  and  $F_T$ .

is released when the molecule leaves the gap between tip and sample. Introducing the activation volume as before and using Eq. (9), we obtain the activation energy

$$\Delta U = \Delta U_0 - \frac{\alpha VF}{2\pi h R}. \quad (20)$$

Inserting this into Eq. (4) and integration leads to

$$\ln P = -\frac{k_0 F_T}{K\nu} (e^{F/F_T} - 1), \quad (21)$$

with  $k_0 \equiv A \exp(-\Delta U_0/k_B T)$  and

$$F_T \equiv \frac{2\pi h R k_B T}{\alpha V}. \quad (22)$$

Please note that  $F_T$  does not depend on Youngs modulus  $E$ .

## B. Results and discussion

As a result, the yield probabilities vs force for different values of the rate  $k_0$  are shown in Figs. 8(a) and 8(b). The same dependencies as calculated with the full molecular model are obtained: The mean yield force increases with increasing  $F_T$  and decreasing  $k_0$  [inset of Fig. 8(b)]. When choosing  $F_T \approx 1.1F_M$ , the curves would be almost identical.

The dependence of the mean yield force on the loading rate can be calculated with Eq. (5),

$$F_0 = F_T \ln \left( \frac{0.693 \nu K}{k_0 F_T} + 1 \right). \quad (23)$$

The mean yield force is proportional to  $\ln \nu$ .

What is the significance of  $F_T$  and what is a reasonable range? Therefore, we consider an activation volume under the tip of  $V = n\lambda^2 h$ . The energy required to compress  $n$  molecules by a distance  $\delta_0$  is  $nE\lambda^2 \delta_0^2 / 2h$ . If we set this energy equal to the thermal energy  $k_B T$ , we obtain

$$k_B T = \frac{nE\lambda^2 \delta_0^2}{2h}. \quad (24)$$

According to Eq. (9) a force  $F = \pi ER \delta_0^2 / h$  would lead to the same compression. Inserting  $\delta_0^2$  of Eq. (24) leads to  $F = 2\pi h R k_B T / V$ , which is equal to  $F_T$  for  $\alpha = 1$ . A thermal energy would lead to the same compression of the activation volume than the force  $F_T$ . For this reason we used the index “ $T$ ” for “thermal force.” With  $h = 4$  nm,  $\alpha = 0.5$ , and  $V = 1$  nm<sup>3</sup>, an upper limit of the thermal force is 8 nN. The lower limit is estimated with  $h = 1$  nm and  $V = 100$  nm<sup>3</sup> to be  $F_T \approx 20$  pN.

Results obtained with the simplified molecular model are formally similar to results reported earlier with a flat stamp model [21]. In the flat stamp model the tip shape is approximated by a planar surface of area  $A_{FS}$ . This leads to a constant pressure  $p = F/A_{FS}$ . Using this model, a probability distribution equal to the one given in Eq. (21) is obtained. Only the thermal force is  $F_T = A_{FS} k_B T / \alpha V$  in the flat stamp model instead of Eq. (22). If both models are applied to the same experimental results, slightly different values of  $\alpha V$  are obtained.

## VI. CONCLUSION

Assuming that the rupture of molecular films induced by an AFM tip is an activated process, we find a universal relation (6) between the loading rate and the force dependence of the activation energy. To calculate the activation energy we suggest two complementary models: A continuum nucleation theory and a discrete molecular model. In the continuum theory the line tension  $\Gamma$  and the spreading pressure  $S$  determine the activation energy. In the molecular theory, the activation volume  $V$  is the relevant microscopic parameter. The full molecular model leads to complicated mathematical expressions. Therefore, a simplified molecular model is proposed. We demonstrate that the simplified model is a good approximation of the full molecular model.

## ACKNOWLEDGMENT

We thank the Deutsche Forschungsgemeinschaft for financial support (Grants Nos. Bu 701/14 and Bu 701/19).

- 
- [1] J. A. N. Zasadzinski, C. A. Helm, M. L. Longo, A. L. Weisenhorn, S. A. C. Gould, and P. K. Hansma, *Biophys. J.* **59**, 755 (1991).
  - [2] A. L. Weisenhorn, M. Egger, F. Ohnesorge, S. A. C. Gould, S. P. Heyn, H. G. Hansma, R. L. Sinsheimer, H. E. Gaub, and P. K. Hansma, *Langmuir* **7**, 8 (1991).
  - [3] S. W. Hui, R. Viswanathan, J. A. Zasadzinski, and J. N. Israelachvili, *Biophys. J.* **68**, 171 (1995).
  - [4] J. Schneider, Y. F. Dufrene, W. R. Barger, and G. U. Lee, *Biophys. J.* **79**, 1107 (2000).
  - [5] T. Viitala and J. Peltonen, *Biophys. J.* **76**, 2803 (1999).
  - [6] A. S. Muresan and K. Y. C. Lee, *Langmuir* **105**, 852 (2001).
  - [7] Y. F. Dufrene and G. U. Lee, *Biochim. Biophys. Acta* **1509**, 14 (2000).
  - [8] H.-J. Butt, M. Jäschke, and W. Ducker, *Bioelectrochem. Bioenerg.* **38**, 191 (1995).
  - [9] B. Cappella and G. Dietler, *Surf. Sci. Rep.* **34**, 1 (1999).
  - [10] A. Jansoff, M. Neitzert, Y. Oberdörfer, and H. Fuchs, *Angew. Chem.* **112**, 3346 (2000).
  - [11] H. Mueller, H.-J. Butt, and E. Bamberg, *J. Phys. Chem.* **104**, 4552 (2000).
  - [12] Y. F. Dufrene, T. Boland, J. W. Schneider, W. R. Barger, and G. U. Lee, *Faraday Discuss.* **111**, 79 (1998).
  - [13] J. Rädler, M. Radmacher, and H. E. Gaub, *Langmuir* **10**, 3111 (1994).
  - [14] I. Burgess, C. A. Jeffrey, X. Cai, G. Szymanski, Z. Galus, and J. Lipkowski, *Langmuir* **15**, 2607 (1999).
  - [15] W. A. Ducker and D. R. Clarke, *Colloids Surf. A* **94**, 275 (1994).
  - [16] S. Manne, J. P. Cleveland, H. E. Gaub, G. D. Stucky, and P. K. Hansma, *Langmuir* **10**, 4409 (1994).
  - [17] M. Jäschke, H.-J. Butt, H. E. Gaub, and S. Manne, *Langmuir* **13**, 1381 (1997).
  - [18] S. J. O’Shea, M. E. Welland, and T. Rayment, *Appl. Phys. Lett.* **60**, 2356 (1992).
  - [19] Y. Kanda, T. Nakamura, and K. Higashitani, *Colloids Surf., A* **139**, 55 (1998).
  - [20] F. Mugele, S. Baldelli, G. A. Somorjai, and M. Salmeron, *J. Phys. Chem.* **104**, 3140 (2000).
  - [21] V. Franz, S. Loi, H. Müller, E. Bamberg, and H.-J. Butt, *Colloids Surf. B* **23**, 191 (2002).
  - [22] K. Kocevar, R. Blinc, and I. Musevic, *Phys. Rev. E* **62**, 3055 (2000).
  - [23] D. Exerova and D. Kashchiev, *Temp. Phys.* **27**, 429 (1986).
  - [24] K. D. Danov, N. Alleborn, H. Raszillier, and F. Durst, *Phys. Fluids* **10**, 131 (1998).



- [25] A. Oron, S. H. Davis, and S. G. Bankoff, *Rev. Mod. Phys.* **69**, 931 (1997).
- [26] B. N. J. Persson, *Sliding Friction. Physical Principles and Applications* (Springer, Berlin, 1998).
- [27] C. Taupin, M. Dvolaitzky, and C. Sauterey, *Biochemistry* **14**, 4771 (1975).
- [28] V. F. Pastushenko, Y. A. Chizmadzhev, and V. B. Arakelyan, *J. Electroanal. Chem.* **104**, 53 (1979).
- [29] W. Harbich and W. Helfrich, *Z. Naturforsch. A* **34A**, 1063 (1979).
- [30] U. Zimmermann, G. Pilwat, A. Péqueux, and R. Gilles, *J. Membr. Biol.* **54**, 103 (1980).
- [31] S. S. Dimitrov and R. K. Jain, *Biochim. Biophys. Acta* **779**, 437 (1984).
- [32] B. Heymann and H. Grubmüller, *Phys. Rev. Lett.* **84**, 6126 (2000).
- [33] D. F. J. Tees, R. E. Waugh, and D. A. Hammer, *Biophys. J.* **80**, 668 (2001).
- [34] K. L. Johnson, *Contact Mechanics* (Cambridge University Press, Cambridge, 1985).
- [35] W. Helfrich, *Phys. Lett.* **50B**, 115 (1974).
- [36] D. V. Zhelev and D. Needham, *Biochim. Biophys. Acta* **1147**, 89 (1993).
- [37] B. V. Derjaguin and A. V. Prokhorov, *J. Colloid Interface Sci.* **81**, 108 (1981).
- [38] B. N. J. Persson and E. Tosatti, *Phys. Rev. E* **50**, 5590 (1994).
- [39] H.-J. Butt, *J. Colloid Interface Sci.* **180**, 251 (1996).
- [40] O. I. Vinogradova, H.-J. Butt, G. E. Yakubov, and F. Feuillebois, *Rev. Sci. Instrum.* **72**, 2330 (2001).
- [41] J. Drelich, *Colloids Surf., A* **116**, 43 (1996).
- [42] T. Pompe and S. Herminghaus, *Phys. Rev. Lett.* **85**, 1930 (2000).
- [43] H.-J. Galla, W. Hartmann, U. Theilen, and E. Sackmann, *J. Membr. Biol.* **48**, 215 (1979).
- [44] M. H. Cohen and D. Turnbull, *J. Chem. Phys.* **31**, 1164 (1959).
- [45] T. A. Fulton and L. N. Dunkleberger, *Phys. Rev. B* **9**, 4760 (1974).
- [46] P. Läger, *Ion Pumps* (Sinauer Associates, New York, 1991).
- [47] R. Zannoni, C. Naselli, J. Bell, G. I. Stegman, and C. T. Seaton, *Phys. Rev. Lett.* **57**, 2838 (1986).
- [48] V. Franz and H.-J. Butt, *J. Phys. Chem. B* **106**, 1703 (2002).
- [49] E. Evans, *Annu. Rev. Biophys. Biomol. Struct.* **30**, 105 (2001).